# Constructing a Radio Telescope for Detecting Jovian Aurora Emissions

Erin Duncan, Dr. Anna DeJong

Christopher Newport University

## 1. Abstract

The purpose of this experiment is to detect Jovian emissions with a 20.1 MHz radio telescope in order to better understand the Jovian aurora, Jupiter’s magnetic field, and how Jupiter interacts with its moon Io to enhance the emission of decametric radio waves. This radio telescope is constructed using blueprints from NASA's Radio JOVE Project, a project designed to provide radio astronomy resources to amateur and professional scientists alike. With this radio telescope, Jovian radio emission data has been gathered over three months, and the results have been compared with Jupiter noise storm predictions to depict the likelihood of storm detection and its correlation with the planetary configuration of Jupiter, Io, and the Earth.

## 2. Introduction

The Jovian aurora is a powerful source of energy, producing 1,000 times more power than the Earth's aurora. Unlike the Earth – whose aurora borealis and aurora australis are produced by solar activity – Jupiter’s aurora is permanent and thought to come from the sulfur and oxygen ions produced by volcanoes on the moon Io, with some auroral activity potentially being affected by solar winds. These charged particles accelerate through Jupiter's magnetosphere along the magnetic field lines towards the northern and southern magnetic poles, where they excite atmospheric particles. When the atmospheric particles return to their normal

state, they release light particles known as photons, which create a visible aurora. The streams of electrons responsible for these aurorae also release radio emissions in the range of 3-40 MHz known as decametric radiation (DAM) which is detectable on Earth with a radio telescope calibrated to this frequency. NASA offers a non-profit kit for building a 20.1 MHz radio telescope called “Radio JOVE,” which is specifically designed for receiving Jupiter’s radio emissions. Radio JOVE antennae intercept energy from Jupiter’s DAM emissions and convert that energy into an electrical signal at the antenna terminals. This weak radio frequency is fed through a transmission line to a direct conversion radio receiver, which amplifies the frequency and converts it to perceptible audio signals, making it possible to record the Jovian DAM on Earth.

**3. Theory**

It is unknown exactly why Jupiter emits radio waves in the frequency range it does, though it hypothesized that the frequency of DAM corresponds to the electron cyclotron frequency of accelerated charged particles in the magnetosphere of Jupiter. This is due to corresponding evidence between the cutoff frequency of the spectrum at 40 MHz, the maximum cyclotron frequency and maximum magnetic field at Jupiter’s surface (Zaĭtsev, 1011). A 20.1 MHz radio telescope can detect and record most of these radio emissions. These converted radio emissions present themselves in two ways: L-burst sounds and S-burst sounds, standing for “long” and “short” bursts respectively. The former is caused as DAM is propagated through space, and the latter is theoretically caused by heightened storm activity on Jupiter’s moon Io as it orbits Jupiter. By plotting the frequencies of L-bursts and S-bursts over time, it is possible to predict Jupiter’s storms. This also allows the possibility to determine any factors that may cause discrepancies in an otherwise routine storm pattern, based on the 10-hour rotation of Jupiter and

Io as it passes through – and interacts with – different longitudinal regions of Jupiter. Researchers have found that when certain regions of Jupiter's longitudes are facing Earth, the likelihood of receiving a decametric noise storm is enhanced. Three longitudinal regions were shown to have this characteristic, labeled A, B, and C. It was found that certain combinations of Jupiter's central meridian longitude and Io position in its orbit around the planet could be significantly related to noise storm reception; these periods of Jupiter-Io interaction are correspondingly referred to as Io-A, Io-B, and Io-C.

## 4. Methods

### 4.1 Receiver Methods

Signals from the antenna are delivered from the antenna terminals to the receiver by a coaxial transmission line. These signals are filtered to reject strong out-of-band interference and are then amplified using a junction field effect transistor (JFET). This transistor and its associated circuitry provide additional filtering and amplify incoming signals by a factor of 10. The receiver input circuit is designed to efficiently transfer power from the antenna to the receiver while developing minimum noise within the receiver itself. The local oscillator (LO) and mixer convert the desired radio frequency signals down to the range of audio frequencies, generating a sinusoidal voltage wave form at a frequency of 20.1 MHz; the exact frequency is set by the front panel tuning control. A low pass filter is used to eliminate interfering signals at nearby frequencies, passing low audio frequencies up to 3.5 kHz and attenuating higher frequencies. Audio amplifiers are used to take the weak audio signal and amplify it enough to drive the signal through a male-to-male auxiliary cable to the mic input on a laptop, which is running Radio-SkyPipe to chart and record the incoming audio signal. The receiver is powered by a 12-volt deep cycle marine battery; the terminals of the battery are connected to the receiver

using a cord with a male adapter with stripped leads. The schematic for the circuit board of the receiver and a block diagram depicting the conversion process of the radio emissions to audio signals can be found in Appendix A.

## 4.2 Antenna Methods

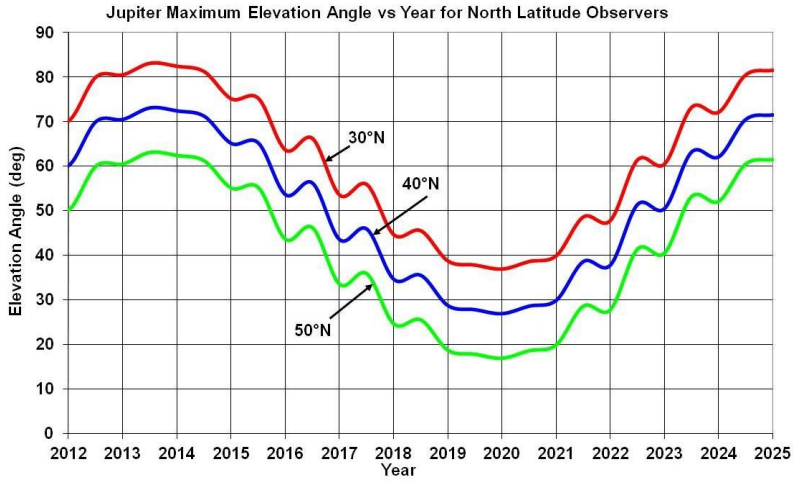


**Figure 4.2.1: Jupiter Elevation Angles for Northern Latitudes**

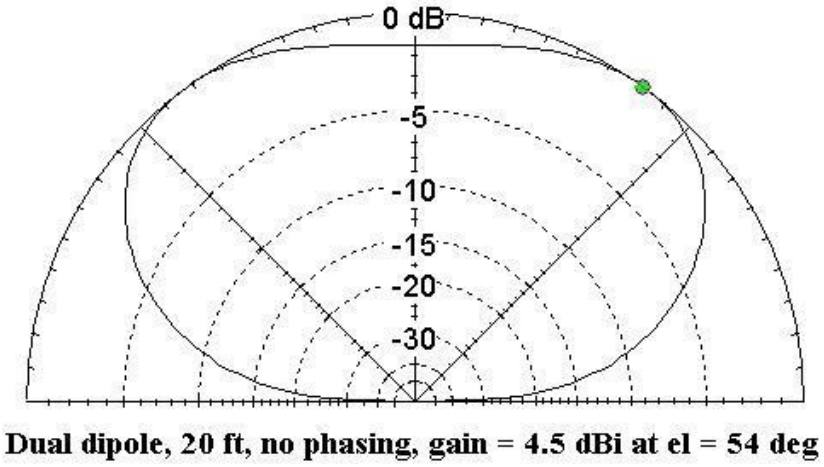


**Figure 4.2.2: 20' Dual Dipole Array Beaming Pattern**

The Jove dual dipole antenna array uses two dipole antennas to achieve almost twice the gain of a single dipole. The direction of the antenna beam can be changed by using varying

lengths of phasing cables or adjusting the height of the antenna. Optimum beam elevation depends upon the latitude of the observer and the declination of Jupiter. Using Figures 4.2.1 and 4.2.2, the optimal height and phasing for the antenna can be found based on the location of the antenna array, which is in King George, Virginia at 38:14:24.8 N 77:11:13.7 W. At 38 N, Jupiter's maximum elevation is approximately 55˚, thus making the most ideal setup the 20' dual dipole array with no phasing. Additional beam pattern diagrams for various configurations can be referenced in Appendix A. The antenna array is erected in a flat, spacious field in a rural area, far away from noise sources such as power lines and buildings that could potentially cause interference. PVC and conduit pipes are used as masts for the antenna array, as it is the most inexpensive and lightweight option. The antenna system is weatherproofed against both rain and cold using preventative draining measures and generous amounts of electrical and self-bonding sealing tape at any electrical junction. Blueprints for the antenna mast system can be found in Appendix A.

**4.3 Radio-Jupiter Pro III**

Radio-Jupiter Pro III (RJP) is a Jupiter noise storm program that offers customizable storm predictions based on the location of the antenna array. The parameters of the antenna (e.g.: 20' with no phasing) can be entered into the program for a predictive sky map, which shows when Jupiter and the Sun will be up and within the beam of the antenna.

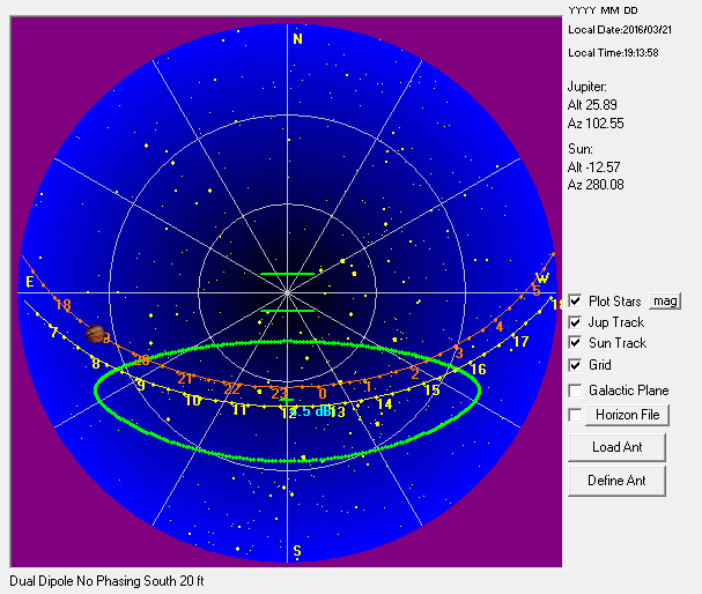


**Figure 4.3.1: Sky Map for 20' No Phasing Configuration**

Figure 4.3.1 shows the sky map feature of RJP, which is configured to the array parameters of a 20' dual dipole oriented E-W with no phasing. This shows the time period in which Jupiter (the path of which is represented by the orange track) or the Sun (represented by the yellow track) passes overhead and is within the beam of the antenna, which is represented by the green ellipse. According to this sky map, Jupiter is overhead and detectable between the approximate hours of 8 pm and 2:30 am EST.

### 4.4 Radio-SkyPipe

Radio-SkyPipe is a licensed software designed for use with the Radio JOVE to collect, store, retrieve, and edit data. This data can be shared real-time with others and includes an integrated messaging system in order to discuss, compare, or troubleshoot any data obtained. This is the primary method used for recording and compiling data. The program records and graphs the audio signal on a strip-chart in real-time while simultaneously recording the audio signal as a wave file. The incoming data is charted as audio signal strength over time. As the intensity of the DAM increases with heightened storm activity, the audio signal strength

increases – that is to say, the more charged particles that are being emitted on Jupiter, the greater the amplitude of the signal strength, varying from low-amplitude galactic background noise to high-amplitude Sun emissions.

## 5. Data

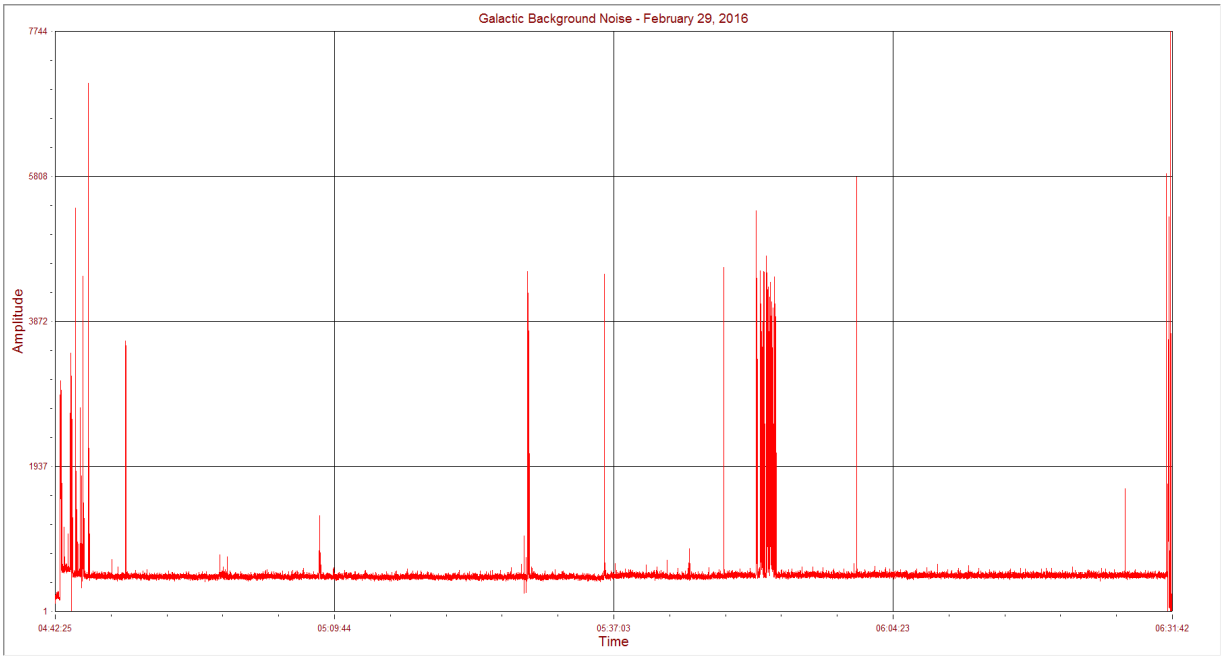


**Figure 5.1: February 29, 2016, 4:42 – 6:31 am EST**

Figure 5.1 is a strip-chart made with Radio-SkyPipe the first night collecting data with the radio telescope. The x-axis represents the local time at which the sample was taken, and the y-axis represents the amplitude of the signal strength. This particular graph is not included to show any conclusive data, rather a learning curve. It was discovered that the array itself is highly sensitive to electronics – particularly the receiver itself, as indicated by loud, crackling interference when a cellphone was moved above it. The hours at which Jupiter is overhead were initially miscalculated and at the time Jupiter had nearly fallen below the horizon, but recording nothing shows a galactic phenomenon called galactic radio noise.

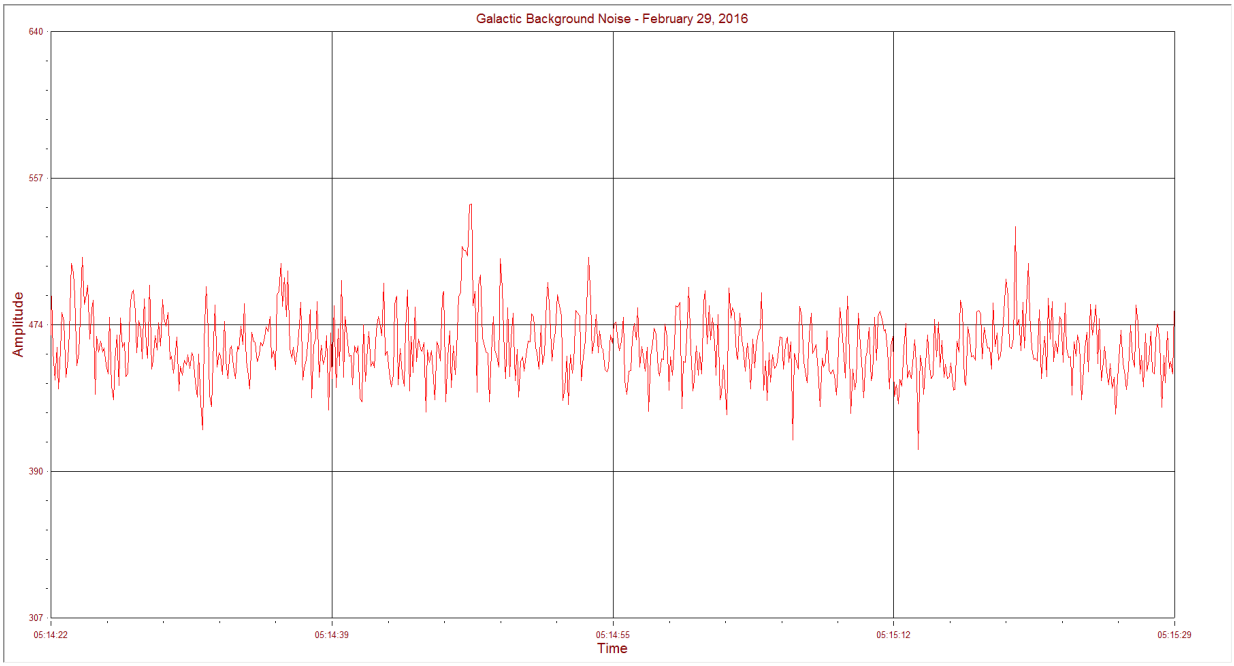


**Figure 5.2: Portion of Figure 5.1 to Show Cosmic Noise**

Galactic radio noise is random noise originating outside of the Earth's atmosphere that is detectable on certain radio receivers. Sources of this noise can include: celestial objects like Quasars, relativistic electrons spiraling in the galactic magnetic field, and meteorites falling and ionizing gases as they burn up in the atmosphere. Galactic background noise peaks in the direction of the center of the Milky Way galaxy, and it is represented on the strip chart as a steady signal devoid of any bursts or sudden change in amplitude with an average range of 432 – 504.

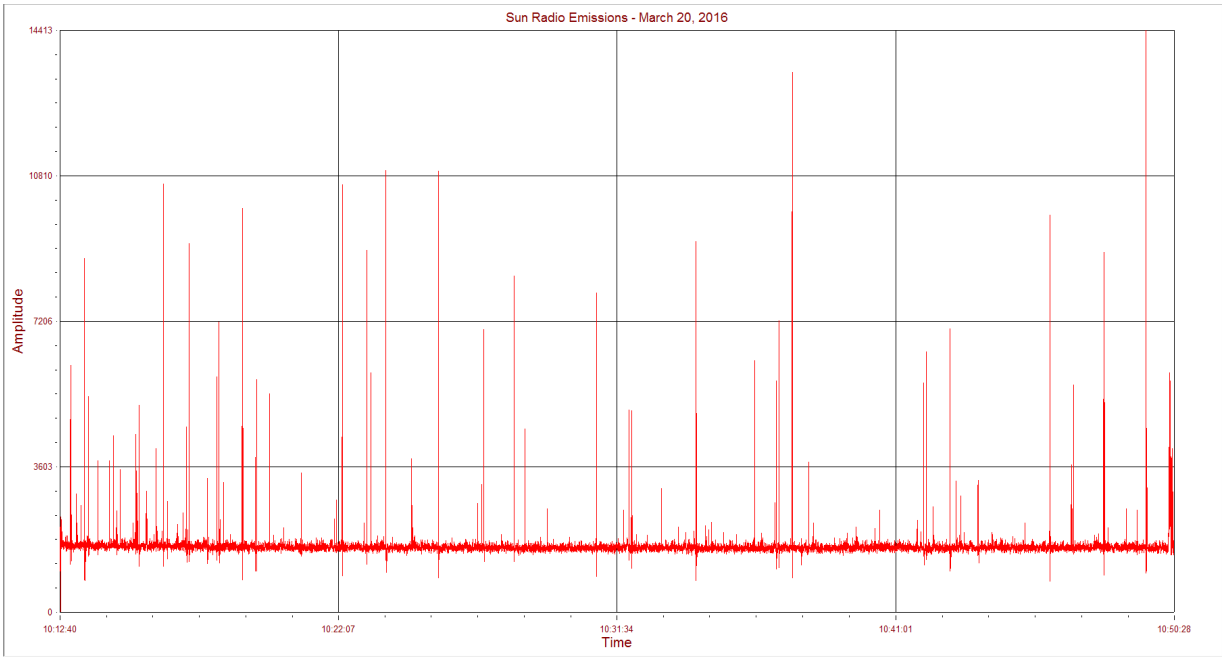


**Figure 5.3: March 20, 2016, 10:12 – 10:50 am EST**

While the radio telescope is configured for receiving Jupiter's emissions, it also has the capability of receiving the Sun's radio emissions. The Sun is much closer and much bigger than Jupiter, and therefore the Sun signal is much stronger than Jupiter's, as shown by the amplitude of the graph of Figure 5.3, which shows a signal strength range of 1500 – 15080. For the purpose of viewing Jupiter, it is important to note that due to the signal strength of the Sun's radio emissions, the Sun's noise would effectively drown out Jupiter's noise. Therefore, if there were ever a point in which both Jupiter and the Sun were overhead, Jupiter's emissions would be negligible or effectively "unheard" over the overpowering Sun's emissions.

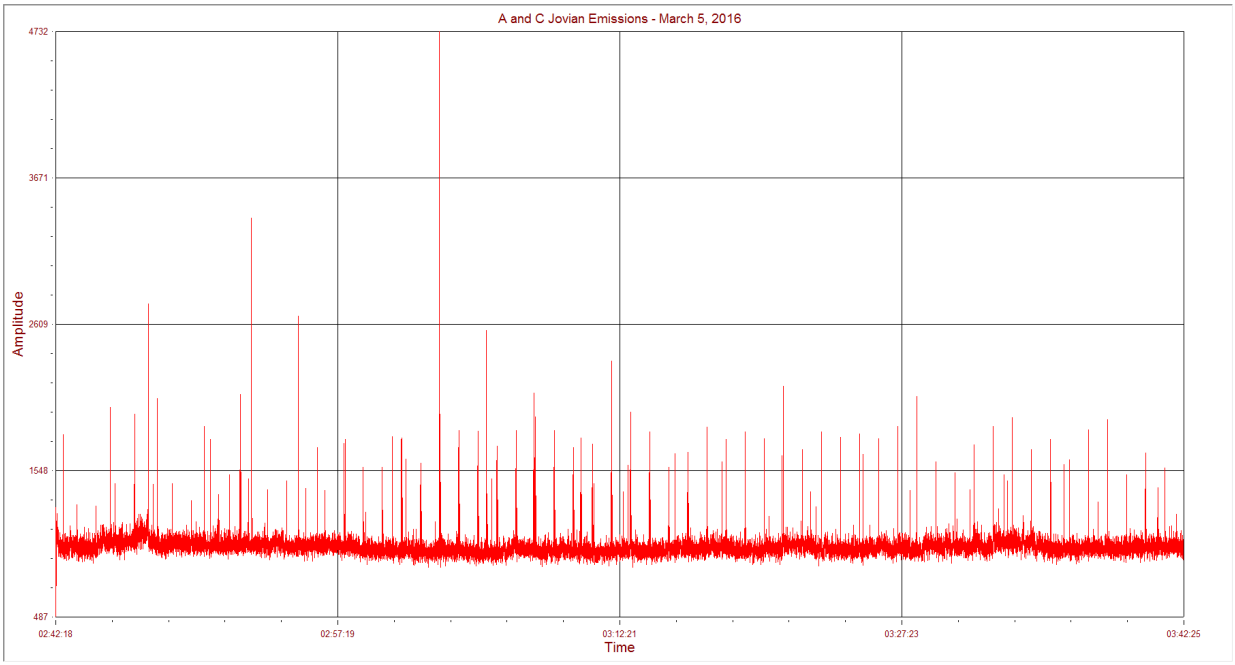


**Figure 5.4: March 5, 2016, 2:42 – 3:42 am EST**

Figure 5.4 shows Jupiter data acquired March 5, 2016 at 2:42 – 3:42 am. This graph shows a low range of periodic signal strengths with few anomalous peaks above the average range of 900 – 2185, with a declining trend in peak signal strength as time progresses. There was an event around 2:46 am, which is indicated by the thin vertical bar at this point on the x-axis. However apparently slight on the full graph, Figure 5.6 shows a closer view of this event over the range of two minutes. According to the storm predictions of Figure 5.5, this was when Jupiter rotated from its A region pointing towards Earth to the C region, with a brief overlap of the periods of the two between 2:44 – 2:46 EST.

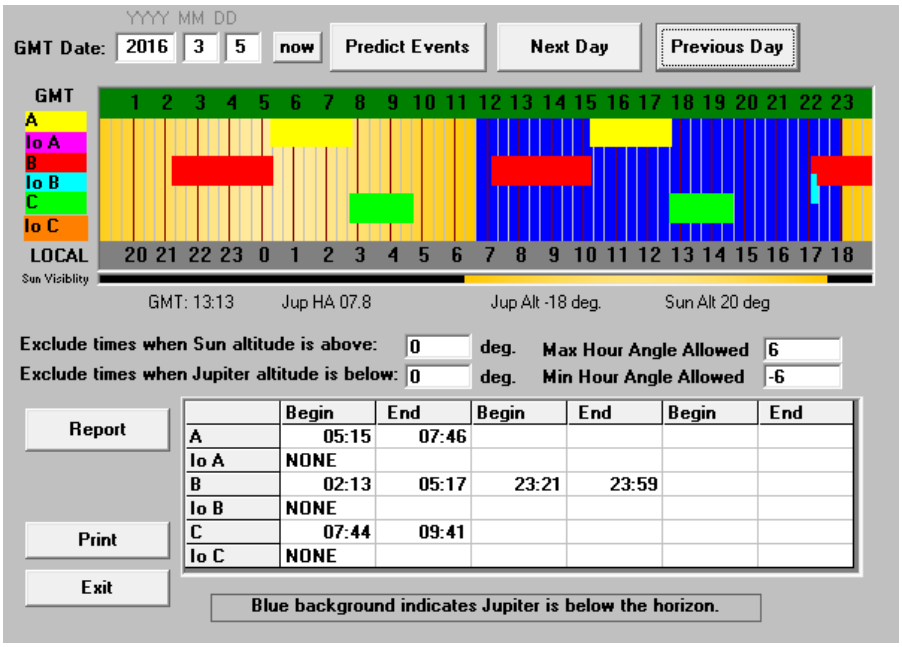


**Figure 5.5: Noise Storm Prediction of Figure 5.4**

Note the Radio-SkyPipe program runs many of its predictions in GMT, so the prediction that the A storm ends at 7:46 and the C storm begins at 7:44 is in GMT, not EST.

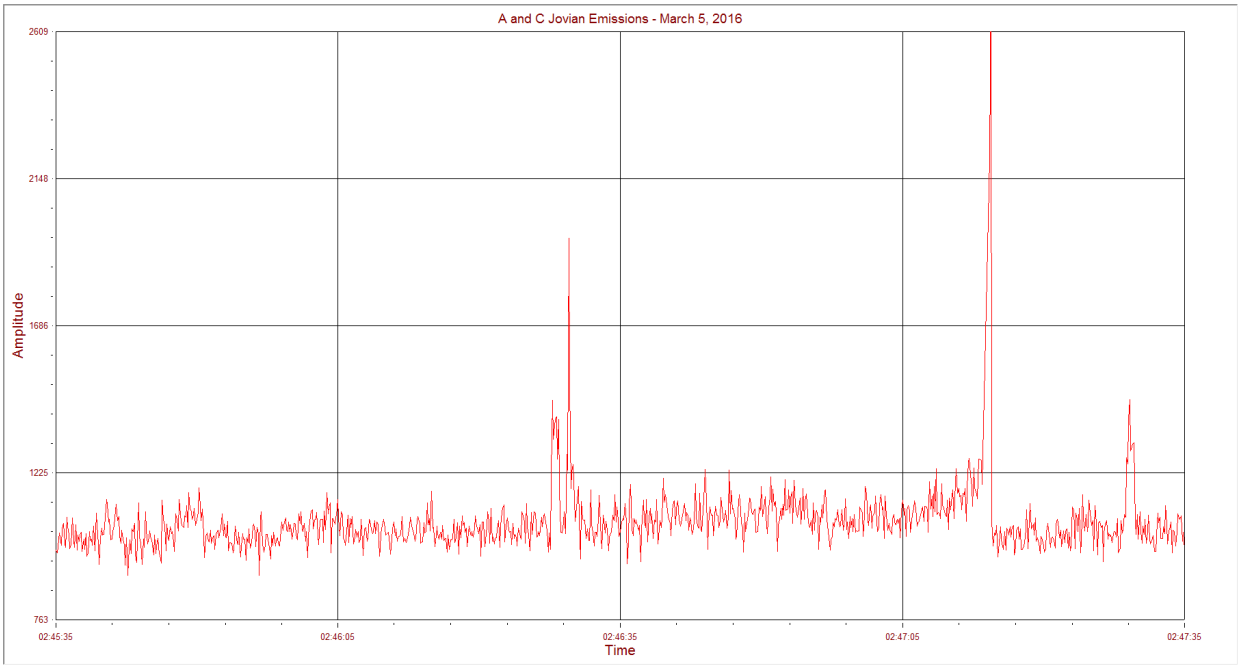


**Figure 5.6: March 5 Event**

## 6. Discussions and Conclusions

The availability of detectable Io-A, Io-B, and Io-C emissions is incredibly limited. While A, B, and C emissions are predictable due to the 10-hour period of Jupiter's rotation, it takes Io about 42.5 hours to complete one orbit around Jupiter, which means it actually moves relatively quickly around a rapidly spinning Jupiter – for reference: the Earth completes one rotation in 365 days and the Moon takes 27 days to orbit the Earth. Due to the rapid nature of Io moving through regions of Jupiter, Io interactions with a longitudinal region that's directed towards Earth are limited, and it's even less likely that that interaction will occur when Jupiter is overhead and in the beam pattern of the antenna. To complicate things even further still, these storm predictions are not an exact science and there is a varying probability of detecting radio storms, depicted by CML-Io plots.

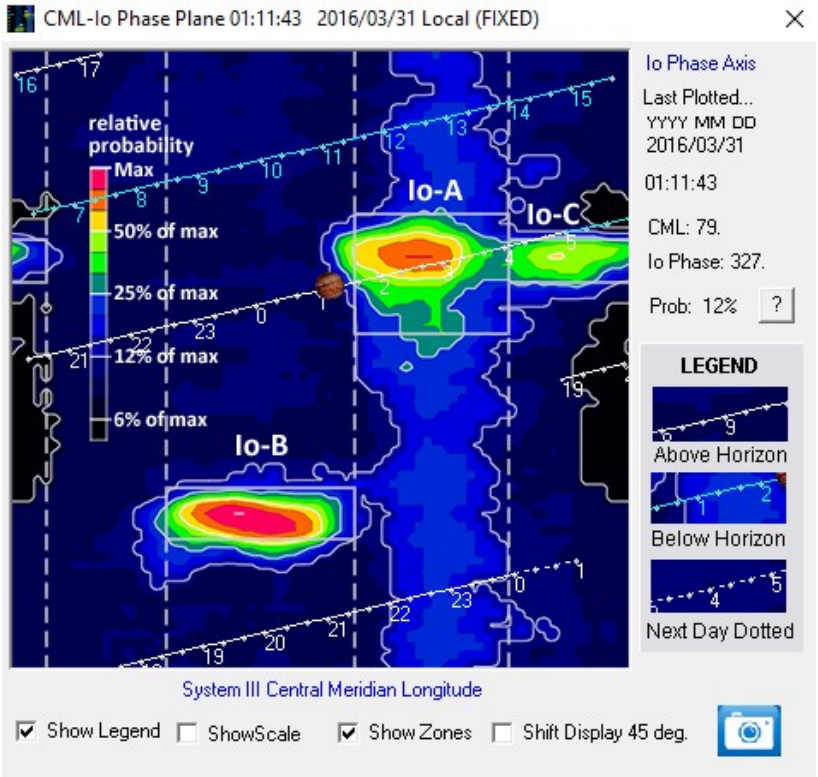

**Figure 6.1: Predictive CML-Io Plot for March 31, 2016**

Figure 6.1 shows a CML-Io plot for March 31, 2016 when Io-A is expected to begin at 1:20 am EST and end at 3:57 am EST. As mentioned in section 4.3, Jupiter is only within the beam of the antenna until 2:30 am EST. The Jupiter icon on the plot follows along a predicted path through areas of noise storm probability. It should be noted that this is an interpretational graphic, and does not actually represent Jupiter moving through high probability regions. The probability of a storm occurring is determined by the surface area of Io that's interacting with longitudinal region A as it orbits around Jupiter. It moves through the probability regions 12%, 25%, 35%, 48%, and finally 54% until Jupiter is no longer within the beam of the antenna and no storm signals can be received at all.

Figure 6.1 shows only one example of many that depicts the general unlikeliness of receiving strong radio storm signals. Due to the sparsity of strong Io interactions, there is no data to represent these interactions, which are responsible for the majority of strong S-burst emissions.

However, ample data has been collected to show the L-burst emissions from Jupiter's persistent aurora. Figure 5.2 and 5.3 show the distinction between two different sources of decametric radio emissions – galactic background noise and the Sun respectively – and how they differ from Jupiter's radio emissions in the average amplitude of signal strength, height of spike activity, periodicity of spikes in signal strength, and general trends towards non-sudden fluctuations of signal strength. Furthermore, the collected Jupiter data can be compared to NASA's Radio JOVE data archive, which contains data uploaded by amateur and professional scientists from around the world.

In the future, this project could be optimized in order to better facilitate the collection of S-burst emissions. The limited amount of data collected was in part due to the remote location of the telescope itself, which restricted data collection to weekends and school breaks. Two possible solutions for remedying this issue are: erecting the radio telescope in a location more accessible to the researcher and designing a system for automated data collection. This would require some housing for the receiver and collecting hardware, as well as a more reliable power source for both. With the design of an automated system, it would ensure that no Io interaction went unrecorded, therefore increasing the likelihood of recording quality S-burst data.

## 7. Appendices

### Appendix A: Radio JOVE Schematics

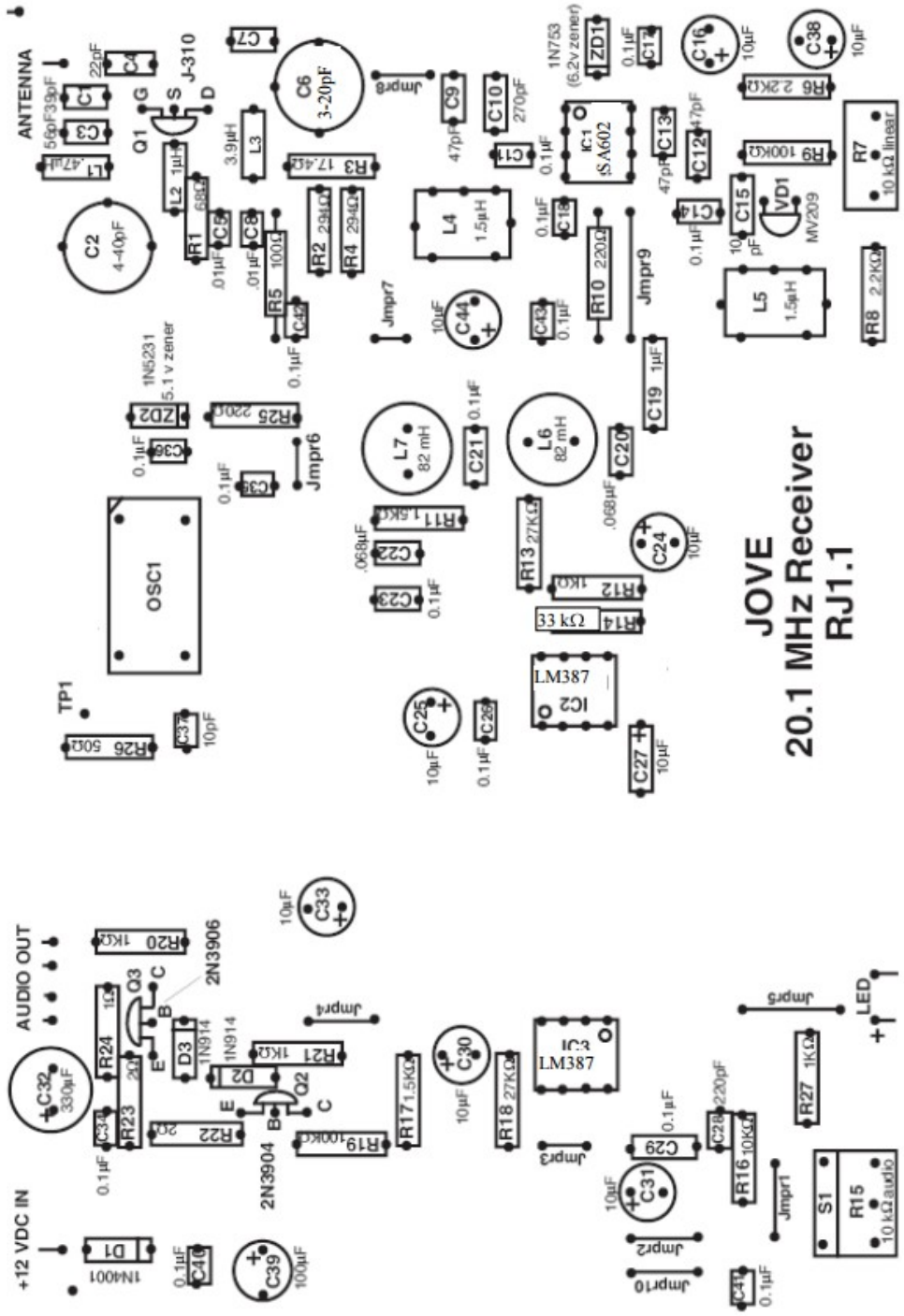


**Figure A.1: Radio JOVE Receiver Schematic**

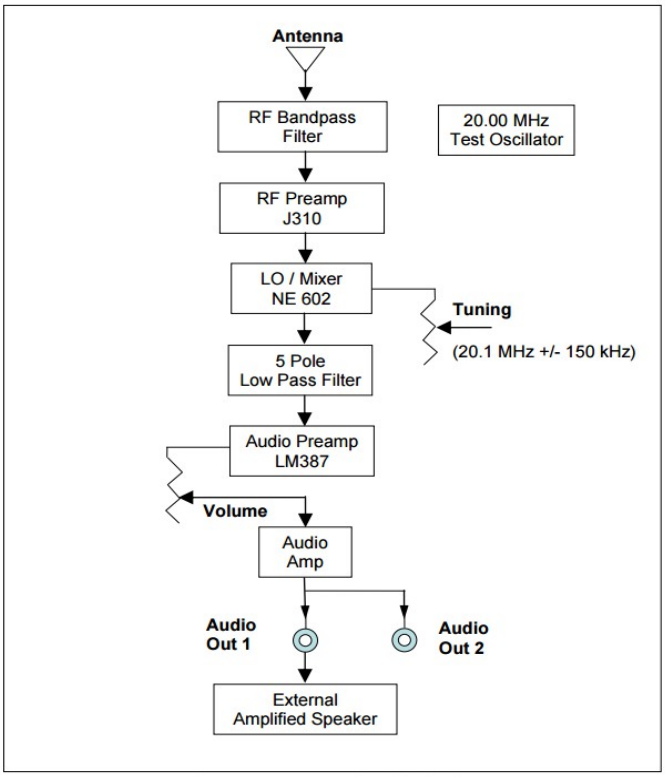


Figure 1. JOVE receiver block diagram

**Figure A.2: Radio JOVE Receiver Block Diagram**

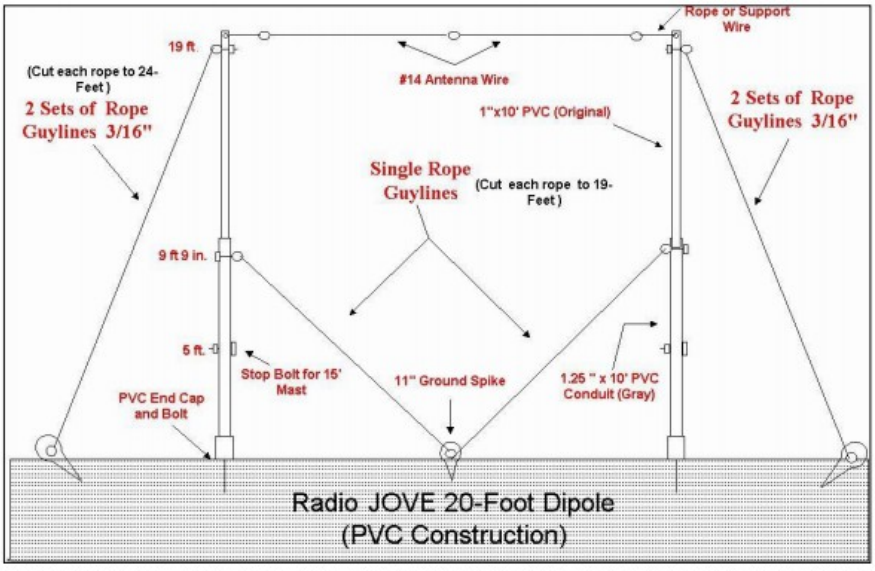


**Figure A.3: Radio JOVE 20' Dipole Antenna Blueprint**

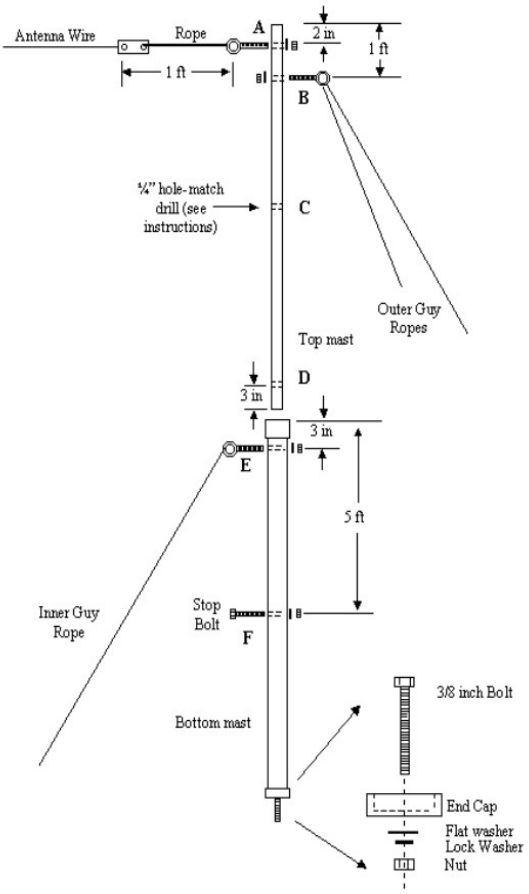
Antenna Wire
Rope
A
2 in
1 ft
1 ft
B
¼" hole- match drill (see instructions)
C
Outer Guy Ropes
Top mast
3 in
D
3 in
E
5 ft
Inner Guy Rope
Stop Bolt
F
Bottom mast
3/8 inch Bolt
End Cap
Flat washer
Lock Washer
Nut

**Figure A.4: Radio JOVE 20’ Dipole Antenna Mast Blueprint**

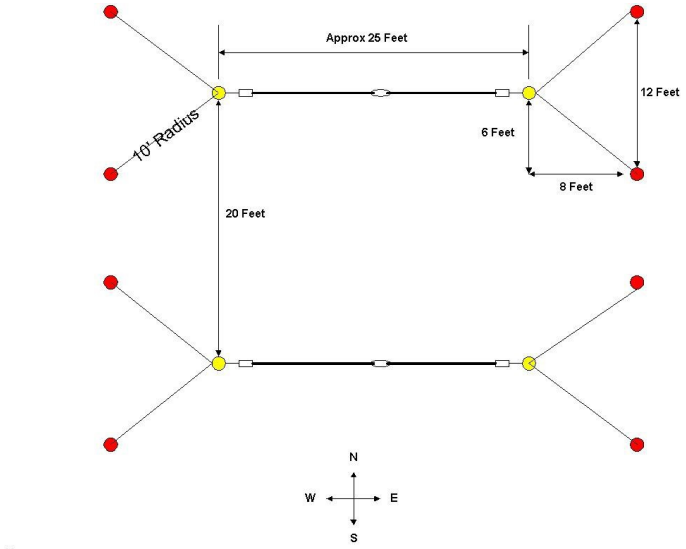


**Figure A.5: Antenna Field Layout for Masts and Guy Stakes**

## Appendix B: Beam Pattern Diagrams for Various Telescope Configurations

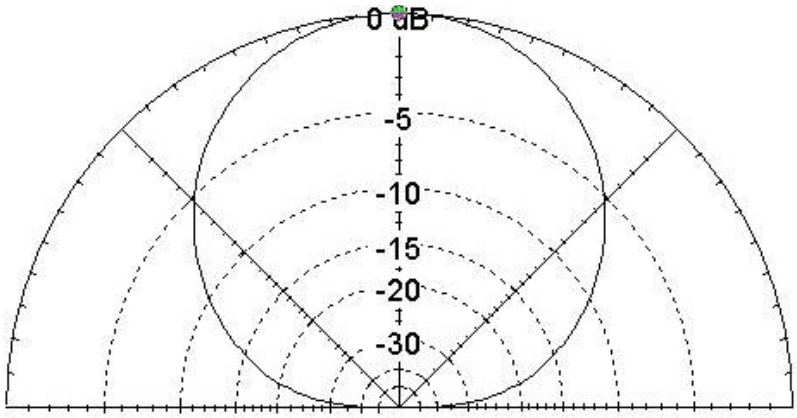


**Dual dipole, 10 ft, no phasing, gain = 7.8 dBi at el = 90**

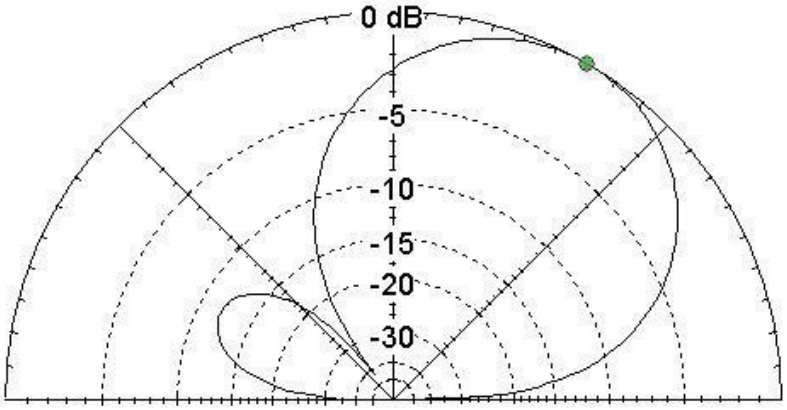


**Dual dipole, 10 ft, 90 deg phasing, gain = 8.5 dBi at el = 60**

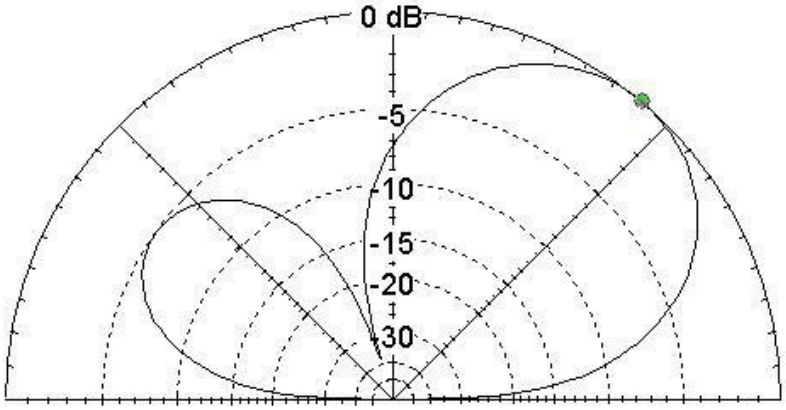


**Dual dipole, 10 ft, 135 deg phasing, gain = 8.5 dBi at el = 50**

**Figure B.1: 10' Dual Dipole Array Beaming Patterns**

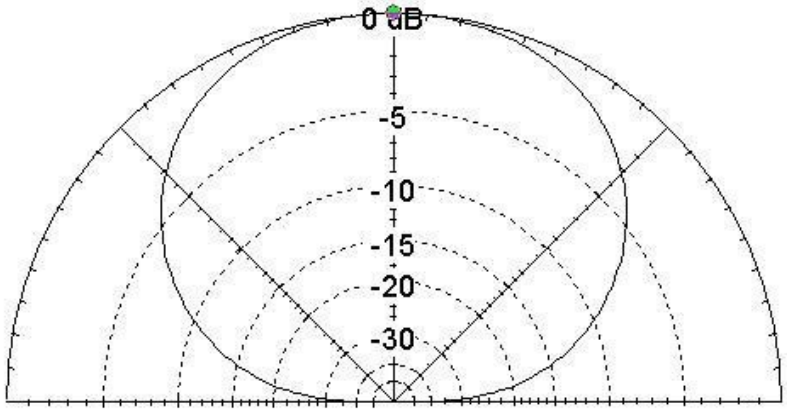


**Dual dipole, 15 ft, no phasing, gain = 6.8 dBi at el = 90 deg**

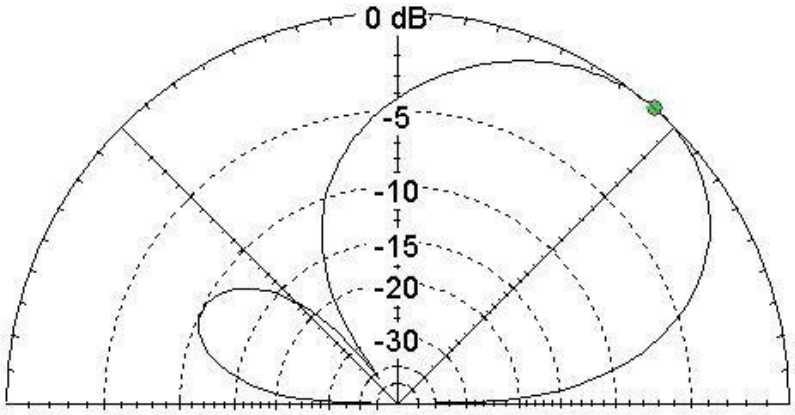


**Dual dipole, 15 ft, 90 deg phasing, gain = 8.7 dBi at el = 49**

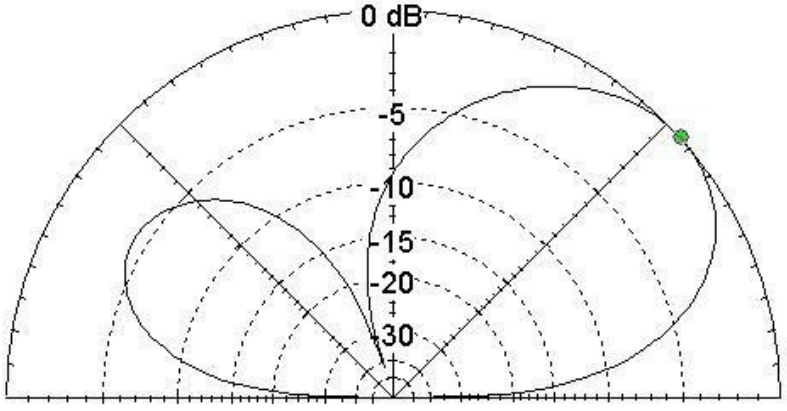


**Dual dipole, 15 ft, 135 deg phasing, gain = 9.1 dBi at el = 42**

**Figure B.2: 15' Dual Dipole Array Beaming Patterns**

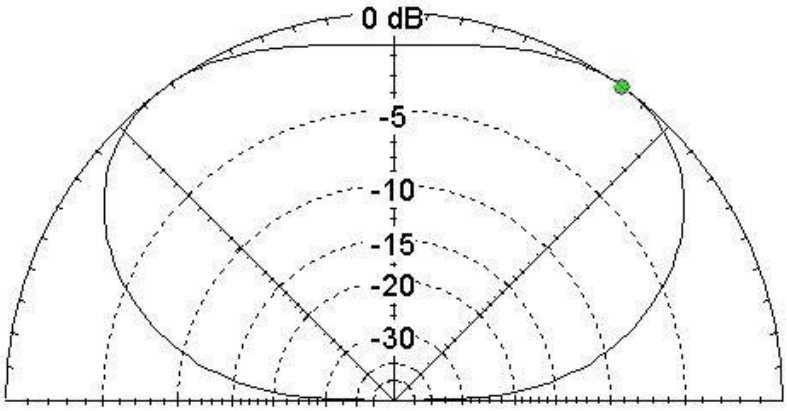


**Dual dipole, 20 ft, no phasing, gain = 4.5 dBi at el = 54 deg**

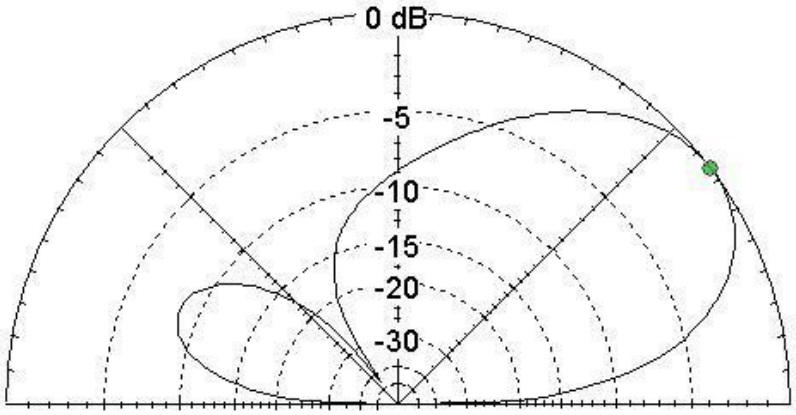


**Dual dipole, 20 ft, 90 deg phasing, gain = 9.1 dBi at el = 37**

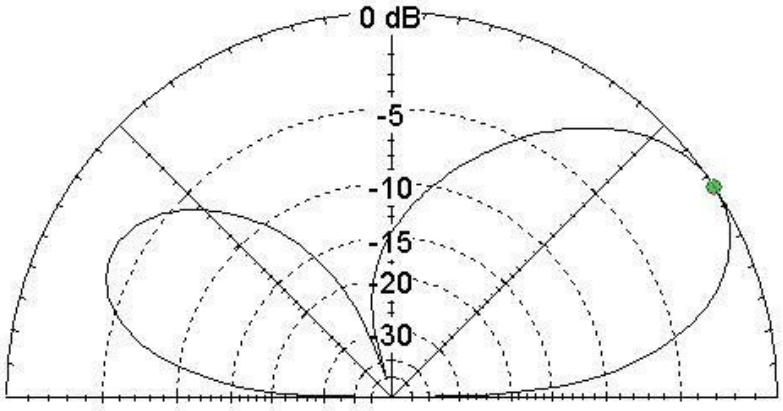


**Dual dipole, 20 ft, 135 deg phasing, gain = 9.5 dBi at el = 33**

**Figure B.3: 20' Dual Dipole Array Beaming Patterns**

**8. Literature Cited**

Belcher, J. W. "The Jupiter-Io Connection: An Alfven Engine in Space." *Science* 238.4824 (1987): 170-76. Web.

Carr, T. D., M. D. Desch, and J. K. Alexander. "Phenomenology of Magnetospheric Radio Emissions." *Physics of the Jovian Magnetosphere* (n.d.): 226-84. Web.

Kivelson, M. G., and C. T. Russell. "Radio Emissions." *Introduction to Space Physics*. Cambridge: Cambridge UP, 1995. 517-19. Print.

Zaĭtsev, V. V., E. Ya Zlotnik, and Vladimir E. Shaposhnikov. "Cyclotron Mechanism of Decameter Radio Emission of Jupiter." *Soviet Physics Uspekhi Sov. Phys. Usp.* 30.11 (1987): 1011. Web.